INTERNATIONAL JOURNAL OF OPTIMIZATION IN CIVIL ENGINEERING
Int. J. Optim. Civil Eng., 2024; 14(3):489-502

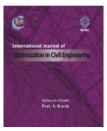

SEISMIC LIFE-CYCLE COST ANALYSIS OF OPTIMALLY DESIGNED STEEL MOMENT FRAMES

S. Gholizadeh[*, †] and S. Tariverdilo
Department of Civil Engineering, Urmia University, Urmia, Iran

[DOI: 10.22068/ijoce.2024.14.3.604]

ABSTRACT

The primary objective of this paper is to assess the seismic life-cycle cost of optimally designed steel moment frames. The methodology of this paper involves two main steps. In the first step, we optimize the initial cost of steel moment frames within the performance-based design framework, utilizing nonlinear static pushover analysis. In the second step, we perform a life cycle-cost analysis of the optimized steel moment frames using nonlinear response history analysis with a suite of earthquake records. We consider content losses due to floor acceleration and inter-story drift for the life cycle cost analysis. The numerical results highlight the critical role of integrating life-cycle cost analysis into the seismic optimization process to design steel moment frames with optimal seismic life-cycle costs.

Keywords: seismic life cycle cost; performance-based design; nonlinear response history analysis; steel moment resisting frame.

Received: 3 September 2024; Accepted: 5 October 2024

1. INTRODUCTION

The primary concern for any structure is ensuring it has adequate seismic resistance to remain functional after an earthquake. To achieve this, performance-based design (PBD) [1] concepts have been developed and integrated into seismic design procedures. The PBD approaches utilize nonlinear structural analysis to assess the nonlinear inelastic response of structures. Furthermore, a key priority for structural engineers is to design cost-effective structures that maintain reliable performance during earthquakes. Consequently, performance-based design optimization (PBDO) techniques have emerged over recent years, with extensive research conducted in this field [2-7]. Metaheuristic algorithms are considered the most suitable technique for solving the PBDO problems [8-10]. In recent

[*]Corresponding author: Department of Civil Engineering, Urmia University, Urmia, P.O. box 165, Iran
[†]E-mail address: s.gholizadeh@urmia.ac.ir (S. Gholizadeh)

decades, a variety of metaheuristic algorithms have been introduced for structural optimization. Drawing inspiration from natural phenomena such as physics, these algorithms have demonstrated greater effectiveness and reliability compared to traditional gradient-based methods in addressing complex and challenging optimization problems [11-13]. Center of Mass Optimization (CMO) algorithm [14] is a physics-based metaheuristic method. It operates on the principle that mass should be balanced around its center of mass in space. Recent studies have shown that CMO is effective in solving PBDO problems for steel moment frames, outperforming some other metaheuristics [14]. In this paper, we apply the CMO to tackle the PBDO problem of steel moment frames.

Economic measures offer crucial insights for decision-makers, allowing the consequences of seismic damage to be quantified in terms of direct and indirect economic losses. Historical earthquakes have shown that while conventional design codes can ensure occupant safety, they may still result in considerable economic losses. Life cycle cost analysis (LCCA) is one of the most effective computational tools for integrating economic considerations into the structural design process [15-17]. Over the past decade, numerous studies have been carried out on the LCCA of steel structures [18-19].

A numerical example of a 12-story steel moment frame was illustrated. The CMO algorithm was employed to derive five optimal designs within the framework of PBD by performing nonlinear static pushover analysis according to FEMA-350 [20]. For these optimal designs, LCCA was performed following the procedures outlined in references [15-17] using nonlinear response history analysis for a suite of 22 records listed in FEMA-P695 [21]. The numerical results indicate that the design with the lowest initial cost is not the most cost-effective in terms of seismic life-cycle cost.

2. PERFORMANCE-BASED DESIGN OPTIMIZATION

According to the PBD approach, structures must meet specific performance objectives for different hazard levels. FEMA-356 [1] defines Immediate Occupancy (IO), Life Safety (LS), and Collapse Prevention (CP) as performance levels, and specifies three hazard levels: earthquakes with probabilities of exceedance of 50%, 10%, and 2% within 50 years. Before assessing seismic performance, geometric and strength constraints must be verified. Geometric constraints should be checked at each joint to ensure the dimensions of beams and columns are consistent. As the strength constraints, the structural members' strength must be verified for gravity loads in accordance with ANSI/AISC 360-16 [22]. If these are met, a nonlinear static pushover structural analysis is conducted to verify the PBD constraints. As per FEMA-350, the confidence level (CL) constraints at the IO and CP performance levels are as follows:

$$CL_{IO} \geq \overline{CL}_{IO} \tag{1}$$

$$CL_{CP} \geq \overline{CL}_{CP} \tag{2}$$

where the minimum allowable confidence level $\overline{CL}_{IO}$ and $\overline{CL}_{CP}$ for IO and CP levels are 50% and 90%, respectively. These correspond to 1.0673% and 5.9385% inter-story drift

[DOI: 10.22068/ijoce.2024.14.3.604]

ratios for pushover analysis and 1.5172% and 5.5116% for nonlinear dynamic analysis.

The confidence level for hazard levels can be computed using the following equation:

$$CL = \emptyset\left(\frac{k\beta_{UT}}{2} - \frac{ln\left(\frac{\gamma\gamma_a D}{\varphi C}\right)}{\beta_{UT}}\right) \tag{3}$$

in which $\emptyset$ is the normal cumulative distribution function; k is the slope of the hazard curve; β_{UT} is an uncertainty measure; γ is a demand variability factor; γ_a is an analysis uncertainty factor; D is the calculated demand; C is the capacity; and φ is a resistance factor [20].

The plastic hinge rotation constraints for each beam and column are evaluated according to ASCE/SEI-41-13 [23] at the IO, LS, and CP performance levels as follows:

$$\theta_{IO} \leq \theta_{all,IO} \tag{4}$$

$$\theta_{LS} \leq \theta_{all,LS} \tag{5}$$

$$\theta_{CP} \leq \theta_{all,CP} \tag{6}$$

where $\theta_{all,IO}$, $\theta_{all,LS}$, and $\theta_{all,CP}$ represent allowable plastic hinge rotation at IO, LS, and CP performance levels, respectively.

To delay column hinging, strong column-weak beam (SCWB) constraints are checked in framing joints in accordance with ANSI/AISC 341-16 [24].

The PBOD problem of steel moment frames is formulated as follows:

$$\text{Minimize: } f(X) = \sum_{i=1}^{ne} \rho_i L_i A_i \tag{7}$$

$$\text{Sobjec to: } g_j(X) \leq 0\ , j = 1, \dots, nc \tag{8}$$

where f represents the structural weight; X denotes the design variables vector; ρ_i, L_i, and A_i are the weight density, length and cross-sectional area of the ith element, respectively; g_j is the jth design constraint; and nc is the total number of design constraints.

3. CENTER OF MASS OPTIMIZATION

The CMO algorithm, introduced in [14], is inspired by the concept of the center of mass in physics. In this algorithm, a population including np randomly selected particles (X_i , $i \in [1,np]$) is generated in design space. The mass of ith particle m_i is determined as follows:

$$m_i = \frac{1}{f(X_i)} \tag{9}$$

Particles are sorted by mass in ascending order and divided into two groups, G1 and G2.

[DOI: 10.22068/ijoce.2024.14.3.604]

The first half are assigned to G1, and the rest to G2. Each particles in G1 is paired with a corresponding ones in G2. The center of mass position and the distance between jth pair of particles in iteration t are determined as follows:

$$X_j^C(t) = \frac{m_j X_j(t) + m_{j+\frac{np}{2}} X_{j+\frac{np}{2}}(t)}{m_j + m_{j+\frac{np}{2}}} \tag{10}$$

$$d_j(t) = \left| X_j(t) - X_{j+\frac{np}{2}}(t) \right| \tag{11}$$

To balance exploration and exploitation in the CMO algorithm, the controlling parameter (CP) is calculated, where t_{max} is the maximum number of iterations and α is a constant.

$$CP(t) = \exp\left(-\frac{5t}{t_{max}}\right) \tag{12}$$

The position of jth couple of particles is updated using the following equations

$$if\ d_j(t) > CP(t) \tag{13}$$

$$X_j(t+1) = X_j(t) - R_1\left(X_j^C(t) - X_j(t)\right) + R_2\left(X_b - X_j(t)\right) \tag{14}$$

$$X_{j+\frac{np}{2}}(t+1) = X_{j+\frac{np}{2}}(t) - R_3\left(X_j^C(t) - X_{j+\frac{np}{2}}(t)\right) + R_4\left(X_b - X_{j+\frac{np}{2}}(t)\right) \tag{15}$$

$$if\ d_j(t) \le CP(t) \tag{16}$$

$$X_j(t+1) = X_j(t) + R_5\left(X_j^C(t) - X_{j+\frac{np}{2}}(t)\right) \tag{17}$$

$$X_{j+\frac{np}{2}}(t+1) = X_{j+\frac{np}{2}}(t) + R_6\left(X_j^C(t) - X_{j+\frac{np}{2}}(t)\right) \tag{18}$$

where R_1 to R_6 are vectors of random numbers in interval [0,1]; and X_b is the best solution.

The CMO algorithm includes a mutation operator to reduce the risk of local optima entrapment. A mutation rate $mr = 0.1$ is used and in iteration t a number between 0 and 1 is randomly selected for each particle in group G1 (X_j , j=1,..., $np/2$).

$$r_j(t) \in [0, 1] \tag{19}$$

$$X_j(t) = \left\{x_{j1}(t) \quad x_{j2}(t) \quad \dots \quad x_{ji}(t) \quad \dots \quad x_{jm}(t)\right\}^{\mathrm{T}} \tag{20}$$

For jth particle, if the selected random number is less than the mutation rate, one randomly selected component will be regenerated in the design space as follows:

$$if\ r_j(t) \le mr \ \rightarrow\ x_{ji}(t) = x_{ji}^L + \mu(t) \times \left(x_{ji}^U - x_{ji}^L\right) \tag{21}$$

[DOI: 10.22068/ijoce.2024.14.3.604]

where μ is a random number in the interval [0, 1] in iteration t; and x_{ij}^{L} and x_{ij}^{U} are lower and upper bounds of x_{ji} in design space.

4. SEISMIC LIFE CYCLE-COST ANALYSIS

The life-cycle cost (LCC) of structures is assessed by accounting for both the initial construction cost and the prospective future costs due to seismic damage from earthquakes over the lifespan of structures. The LCC includes repairing damage to structural and non-structural components, loss of contents, injuries, fatalities, and other associated costs [25]. In this study, the calculation of the LCC of steel moment frames incorporates the losses of contents resulting from inter-story drift ratio (ISDR) and floor acceleration (FA), while the other mentioned components are excluded. The initial cost of a structure is directly linked to the cost of its structural components. In this work, the cost per unit weight of steel moment frames is normalized to one, and the structural weight represents the initial cost [26]. The LCC of structures can be calculated using the following equation:

$$LCC(X) = C_{ISDR}(X) + C_{FA}(X) \tag{22}$$

where C_{ISDR} and C_{FA} are the loss of contents costs due to ISDR and FA, respectively.

To quantify the LCC, it is necessary to determine the cost of exceeding certain damage states as a percentage of the initial cost. Table 1 provides the relationships between these damage states and the corresponding values of inter-story drift ratio and floor acceleration [27-28]. The methodology proposed in [15-17] is a robust tool for assessing the LCC of structures. This approach incorporates the Poisson distribution to model earthquake occurrences and assumes that structures will be promptly retrofitted following an earthquake. Consequently, the calculations for C_{ISDR} and C_{FA} are as follows:

Table 1: Damage state limits

Damage state	Mean damage index (*MDI*)	*ISDR* (%)	*FA* (*g*)
None	0.000	$ISDR \leq 0.2$	$FA \leq 0.05$
Slight	0.005	$0.2 < ISDR \leq 0.5$	$0.05 < FA \leq 0.10$
Light	0.050	$0.5 < ISDR \leq 0.7$	$0.10 < FA \leq 0.20$
Moderate	0.200	$0.7 < ISDR \leq 1.5$	$0.20 < FA \leq 0.80$
Heavy	0.450	$1.5 < ISDR \leq 2.5$	$0.80 < FA \leq 0.98$
Major	0.800	$2.5 < ISDR \leq 5.0$	$0.98 < FA \leq 1.25$
Collapse	1.000	$5.0 < ISDR$	$1.25 < FA$

$$C_{ISDR}(X) = \frac{1}{\lambda} \times \left(1 - e^{-\lambda \times t}\right) \times f(X) \times \sum_{i=1}^{7} MDI_i \times P_{ISDR.i} \tag{23}$$

$$C_{FA}(X) = \frac{1}{\lambda} \times \left(1 - e^{-\lambda \times t}\right) \times f(X) \times \sum_{i=1}^{7} MDI_i \times P_{FA.i} \tag{24}$$

[DOI: 10.22068/ijoce.2024.14.3.604]

where λ denotes the annual discount rate; t is the service life of the structure; MDI_i is the mean damage index of ith damage state; $P_{ISDR.i}$, and $P_{FA.i}$ represent the probabilities of exceedance of ith damage state for inter-story drift ratio and floor acceleration, respectively.

5. METHODOLOGY

This paper proposes a methodology that consists of two steps. In the first step, the PBDO process optimizes the initial cost using the CMO algorithm by performing a nonlinear static pushover analysis. Throughout the optimization process, the beam and column sections are chosen from the W-shaped sections detailed in Table 2.

Table 2: Available W-shaped sections

Columns				Beams			
No.	Profile	No.	Profile	No.	Profile	No.	Profile
1	W14×48	13	W14×257	1	W12×19	13	W21×50
2	W14×53	14	W14×283	2	W12×22	14	W21×57
3	W14×68	15	W14×311	3	W12×35	15	W24×55
4	W14×74	16	W14×342	4	W12×50	16	W21×68
5	W14×82	17	W14×370	5	W18×35	17	W24×62
6	W14×132	18	W14×398	6	W16×45	18	W24×76
7	W14×145	19	W14×426	7	W18×40	19	W24×84
8	W14×159	20	W14×455	8	W16×50	20	W27×94
9	W14×176	21	W14×500	9	W18×46	21	W27×102
10	W14×193	22	W14×550	10	W16×57	22	W27×114
11	W14×211	23	W14×605	11	W18×50	23	W30×108
12	W14×233	24	W14×665	12	W21×44	24	W30×116

In the second step, the LCC of the optimized structures is evaluated using the procedure outlined in Section 4. In the LCCA process, nonlinear response history analyses are performed using a set of 22 ground motion records listed in Table 3 [21] to accurately evaluate the seismic response of the structures.

Table 3: Ground motion records

Name	Year	Record Station	Name	Year	Record Station
Northridge	1994	Beverly Hills - Mulhol	Landers	1992	Coolwater
Northridge	1994	Canyon Country-WLC	Loma Prieta	1989	Capitola
Duzce, Turkey	1999	Bolu	Loma Prieta	1989	Gilroy Array #3
Hector Mine	1999	Hector	Manjil, Iran	1990	Abbar
Imperial Valley	1979	Delta	Superstition Hills	1987	El Centro Imp. Co.
Imperial Valley	1979	El Centro Array #11	Superstition Hills	1987	Poe Road (temp)
Kobe, Japan	1995	Nishi-Akashi	Cape Mendocino	1992	Rio Dell Overpass
Kobe, Japan	1995	Shin-Osaka	Chi-Chi, Taiwan	1999	CHY101
Kocaeli, Turkey	1999	Duzce	Chi-Chi, Taiwan	1999	TCU045
Kocaeli, Turkey	1999	Arcelik	San Fernando	1971	LA - Hollywood Stor
Landers	1992	Yermo Fire Station	Friuli, Italy	1976	Tolmezzo

[DOI: 10.22068/ijoce.2024.14.3.604]

In this study, three hazard levels with 50%, 10%, and 2% probability of exceedance in 50 years are considered according to the Iranian seismic design code [29] for soil type III in a very high seismicity region, as shown in Fig. 1. The nonlinear static and dynamic structural analyses are conducted using OpenSees [30] platform.

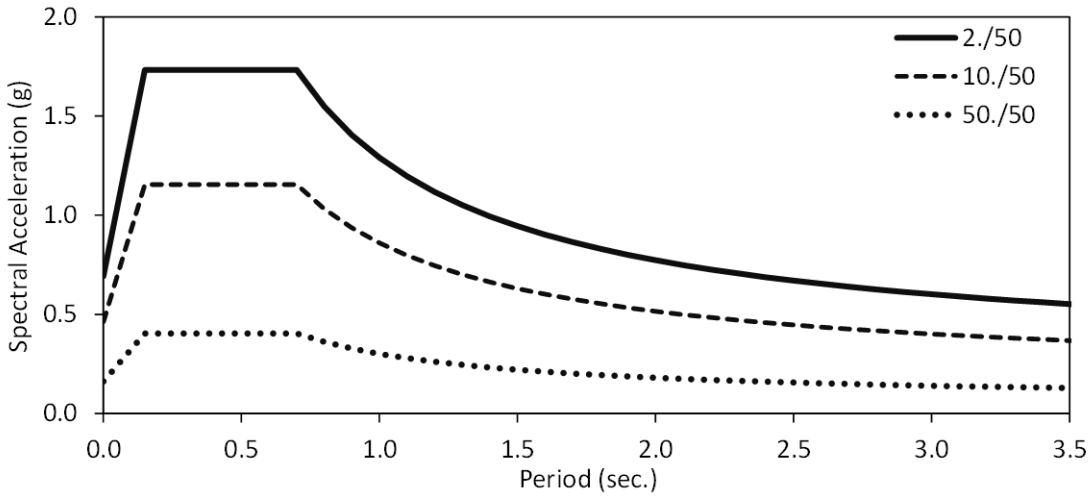

Figure 1. Acceleration response spectra

During the PBDO process, the target displacement for each design candidate is determined using the displacement coefficient method [1] and the acceleration spectra illustrated in Fig. 1. Additionally, for the LCCA, it is essential to determine the dynamic nonlinear response of structures at three seismic performance levels. To achieve this, three nonlinear response history analyses must be conducted for each record, amplitude-scaled to the 5%-damped target acceleration response spectra of the three hazard levels, as shown in Fig. 1, following the procedure outlined in ASCE/SEI-41-13 [23]. Consequently, performing the LCCA requires a total of 66 nonlinear response history analyses.

6. NUMERICAL RESULTS

Figure 2 illustrates the 12-story steel moment frame and its element groupings studied in this paper. A uniform dead load of 2500 kg/m and a live load of 1000 kg/m are applied to all beams. In the numerical model of the steel moment frame, the influence of panel zones is disregarded. The structural components are represented using fiber force-based nonlinear beam-column elements in OpenSees [30]. Moreover, rigid diaphragms are applied to each floor, and P-Delta effects are incorporated into the structural analyses. The type of connection taken into account is welded unreinforced flanges with welded webs [20].

A bilinear behavior is assumed for the materials that exhibit kinematic hardening, characterized by a strain hardening slope of 3%. The yielding stress of the material is set at 344.74 MPa, while the modulus of elasticity is specified as 200 GPa. For nonlinear response history analysis, the Rayleigh damping model is utilized with a constant damping ratio of 2.0% for both the first and third modes [31].

[DOI: 10.22068/ijoce.2024.14.3.604]

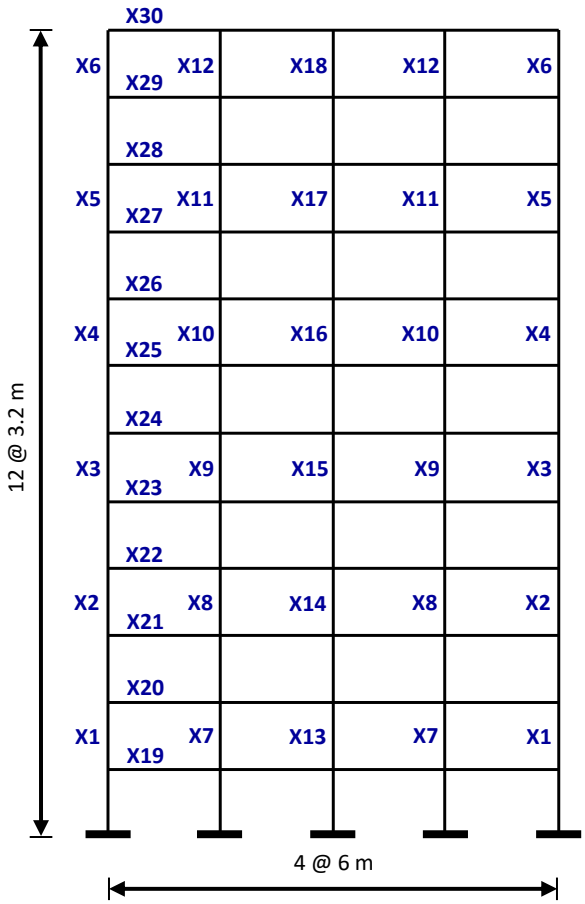

Figure 2. 12-story steel moment frame

6.1 Optimization results

The optimization problem of the 12-story steel moment frame involves 30 design variables comprising 18 variables for columns and 12 variables for beams. The PBDO process is carried out using nonlinear static pushover analysis. The CMO metaheuristic algorithm is employed to perform the optimization. Throughout the optimization process, a total of 100 particles are utilized over a total number of 100 iterations. In this paper, 30 independent optimization runs are conducted and the five best optimal designs obtained are presented in Table 4.

The numerical results of Table 4 reveal that the structural weight of the optimal design I, identified as the best design, is 39290.85 kg. The structural weights of the optimal designs II, III, IV, and V are respectively 4.14%, 4.46%, 4.54%, and 5.12% heavier than the best design.

Figs. 3 and 4 illustrate the inter-story drift ratio profile and plastic rotation demand-to-capacity ratio (DCR) at IO, LS, and CP seismic performance levels for optimal design I. It is evident that the ISDR constraint at the IO performance level dominates the optimal design. Although similar results are observed for the other optimal designs, they are omitted here for brevity.

[DOI: 10.22068/ijoce.2024.14.3.604]

Table 4: Optimization results for 12-story steel moment frame

Design variables	Optimal Designs				
	I	II	II	IV	V
X1	W14×132	W14×132	W14×132	W14×132	W14×132
X2	W14×132	W14×132	W14×132	W14×132	W14×132
X3	W14×68	W14×68	W14×68	W14×68	W14×68
X4	W14×48	W14×53	W14×53	W14×53	W14×53
X5	W14×48	W14×48	W14×48	W14×48	W14×48
X6	W14×48	W14×48	W14×48	W14×48	W14×48
X7	W14×132	W14×132	W14×132	W14×132	W14×132
X8	W14×132	W14×132	W14×132	W14×132	W14×132
X9	W14×82	W14×82	W14×82	W14×82	W14×82
X10	W14×74	W14×74	W14×74	W14×74	W14×74
X11	W14×53	W14×74	W14×68	W14×74	W14×74
X12	W14×48	W14×48	W14×53	W14×48	W14×48
X13	W14×132	W14×132	W14×132	W14×132	W14×132
X14	W14×132	W14×132	W14×132	W14×132	W14×132
X15	W14×82	W14×82	W14×82	W14×82	W14×132
X16	W14×74	W14×74	W14×74	W14×74	W14×68
X17	W14×53	W14×68	W14×68	W14×74	W14×68
X18	W14×48	W14×53	W14×53	W14×48	W14×53
X19	W21×44	W18×40	W21×44	W21×44	W21×44
X20	W18×40	W21×44	W21×44	W21×44	W21×44
X21	W18×40	W21×44	W21×44	W21×44	W21×44
X22	W18×40	W21×44	W21×44	W21×44	W21×44
X23	W18×40	W18×40	W18×40	W18×40	W18×40
X24	W18×40	W18×40	W18×40	W18×40	W18×40
X25	W18×35	W18×40	W18×40	W18×40	W18×35
X26	W18×35	W18×35	W18×35	W18×35	W18×35
X27	W12×35	W18×35	W18×35	W18×35	W18×35
X28	W12×35	W18×35	W18×35	W18×35	W18×35
X29	W12×22	W12×35	W12×35	W12×35	W12×35
X30	W12×22	W12×22	W12×22	W12×22	W12×22
$f(X)$ (kg)	39290.85	40919.59	41046.00	41075.17	41304.49

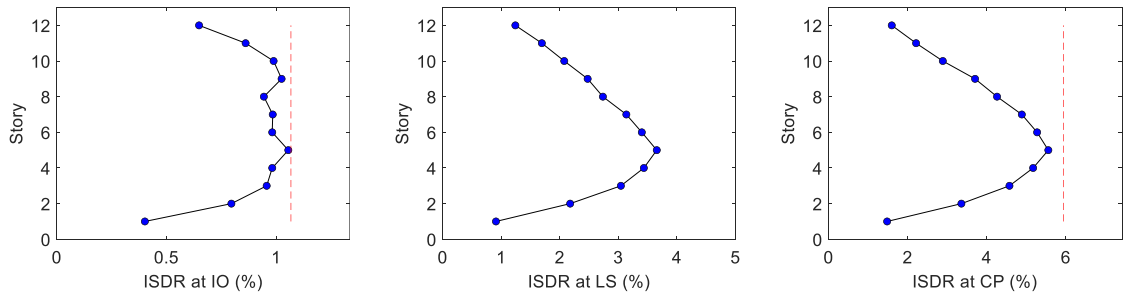

Figure 3. ISDR profiles of the optimal design I at seismic performance levels obtained through nonlinear static pushover analysis

[DOI: 10.22068/ijoce.2024.14.3.604]

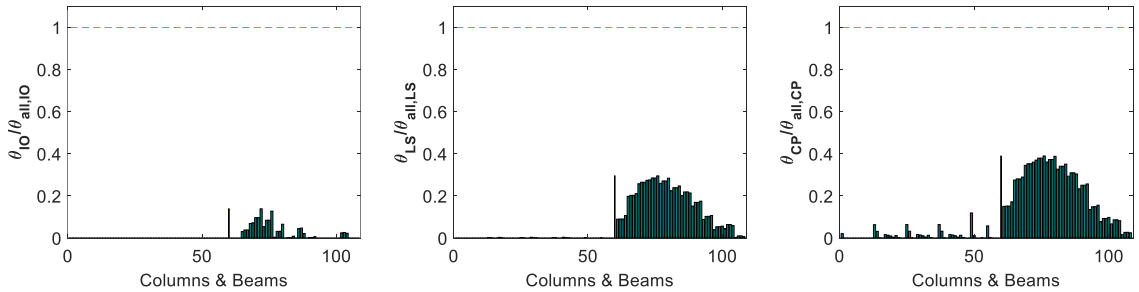

Figure 4. Plastic rotation DCRs of the optimal design I at seismic performance levels obtained through nonlinear static pushover analysis

6.2 Life-cycle cost analysis

The LCCA is performed for all the optimal designs. To this end, nonlinear dynamic responses of the optimal designs are evaluated by conducting nonlinear response history analyses using a set of ground motion records in Table 3. The loss of contents costs due to ISDR and FA, together with the LCCA of all the optimal designs are presented in Table 5.

Table 5: Optimization results for 12-story SMF

Cost (kg)	Optimal Designs				
	I	II	III	IV	V
$C_{ISDR}(X)$	23181.28	17749.01	19609.73	18895.48	21076.21
$C_{FA}(X)$	34667.35	36710.33	36878.62	37094.11	37297.14
$LCC(X)$	57848.63	54459.34	56488.35	55989.59	58373.35

Table 5 shows that the optimal design II has the lowest LCC. The LCCs of the optimal designs I, III, IV, and V are higher by 6.22%, 3.73%, 2.81%, and 7.19%, respectively.

Figs. 5 and 6 depict the inter-story drift ratio profile and plastic rotation demand-to-capacity ratio (DCR) at IO, LS, and CP seismic performance levels for optimal design II obtained by performing nonlinear response history analysis. It is evident that the ISDR constraint at the CP performance level dominates the optimal design. Although similar results are observed for the other optimal designs, they are omitted here for brevity.

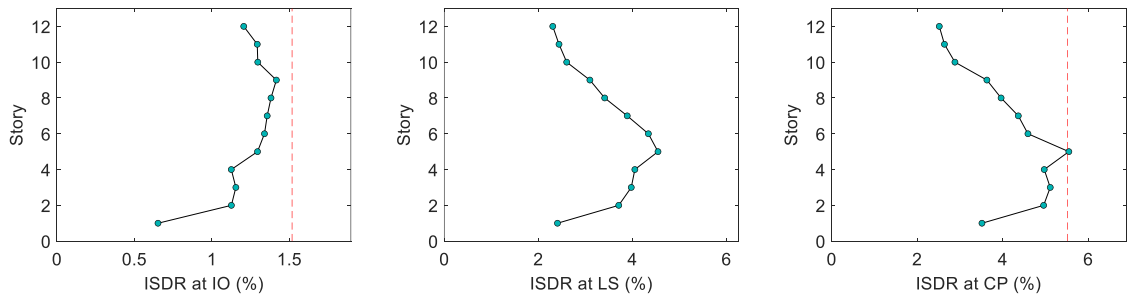

Figure 5. ISDR profiles of the optimal design II at seismic performance levels obtained through nonlinear response history analysis

[DOI: 10.22068/ijoce.2024.14.3.604]

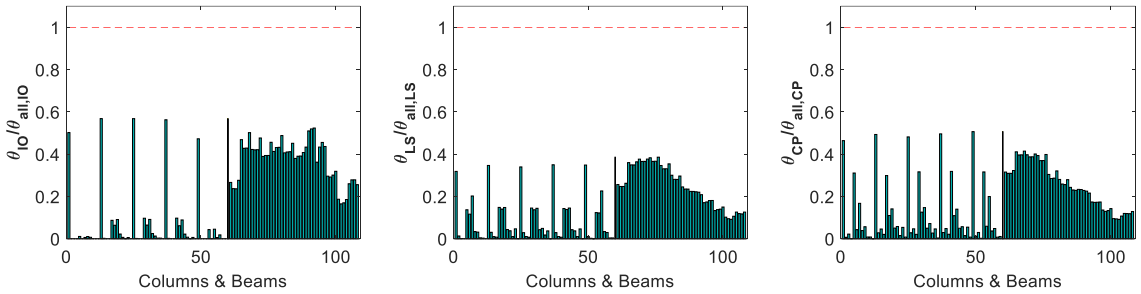

Figure 6. Plastic rotation DCRs of the optimal design II at seismic performance levels obtained through nonlinear response history analysis

The results in Table 5 indicate that the difference in C_{ISDR} between the optimal design II and the other designs is more significant than that of the C_{FA}. This implies that the ISDR is the most influential nonlinear structural response affecting the LCC of the 12-story steel moment frame. Fig. 7 compares the ISDRs of all optimal designs at IO and CP performance levels, obtained through nonlinear response history analysis. It is evident that optimal design I violates the ISDR constraint at the IO performance level. Furthermore, only optimal design II satisfies the ISDR constraint at the CP performance level, while all the other designs violate this constraint.

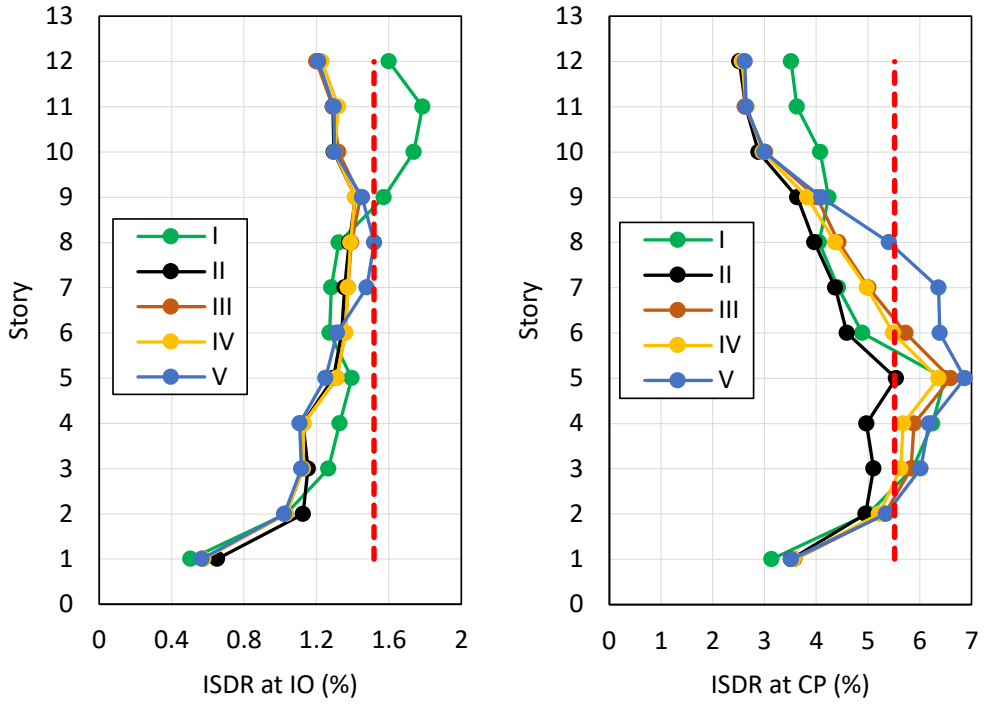

Figure 7. ISDR profiles of all optimal designs at IO and CP performance levels obtained through nonlinear response history analysis

[DOI: 10.22068/ijoce.2024.14.3.604]

7. CONCLUSIONS

This paper focuses on evaluating the seismic life-cycle cost of optimally designed steel moment frames. The methodology comprises two stages. Firstly, the initial cost optimization of steel moment frames is accomplished within a performance-based design framework, employing nonlinear static pushover analysis. Secondly, a life-cycle cost analysis of the optimized steel moment frames is performed using nonlinear response history analysis with a suite of strong ground motion records. For the life-cycle cost analysis, content losses arising from floor acceleration and inter-story drift are taken into account. The findings of this study highlight the importance of incorporating both initial and life-cycle costs in the design optimization process. By focusing on performance-based design, we ensure that the structures not only meet safety and performance criteria but also minimize economic losses over their lifespan. The main findings of this paper can be outlined as follows:

- A design that minimizes initial costs may not always be the optimal choice when considering life-cycle costs. It is essential to evaluate both initial and life-cycle costs to ensure that the chosen design is truly the best option over time.
- Among the factors of nonlinear response history inter-story drift ratio and floor acceleration, the inter-story drift ratio has a more significant impact on the life-cycle cost of steel moment frames.
- The optimal design with the minimum life-cycle cost meets the inter-story drift ratio constraints at the specified seismic performance levels, whereas the other designs fail to satisfy these constraints.

In conclusion, this study provides a comprehensive framework for the seismic performance-based design optimization of steel moment frames, integrating initial cost optimization with life-cycle cost analysis. The proposed approach not only enhances the economic efficiency of the structures but also contributes to their overall performance in seismic regions.

[DOI: 10.22068/ijoce.2024.14.3.604]

REFERENCES

1. FEMA-356, *Prestandard and Commentary for the Seismic Rehabilitation of Buildings*. Federal Emergency Management Agency, Washington DC, 2000.
2. Kaveh A, Farahmand Azar B, Hadidi A, Rezazadeh Sorochi F, Talatahari S. Performance-based seismic design of steel frames using ant colony optimization. *J Constr Steel Res* 2010; **66**: 566–74.
3. Kaveh A, Laknejadi K, Alinejad B. Performance-based multi-objective optimization of large steel structures. *Acta Mech* 2012; **232**: 355–69.
4. Kaveh A, Zakian P. Performance based optimal seismic design of RC shear walls incorporating soil–structure interaction using CSS algorithm. *Int J Optim Civil Eng* 2012; **2**: 383–405.
5. Liang JC, Li LJ, He JN. Performance-based multi-objective optimum design for steel structures with intelligence algorithms. *Int J Optim Civil Eng* 2015; **5**: 79–101.

6. Rahami H, Mohebian P, Mousavi M. Performance-based connection topology optimization of unbraced and X-braced steel frames. *Int J Optim Civil Eng* 2017; **7**:451–68.
7. Ganjavi B, Hajirasouliha I. Optimum performance-based design of concentrically braced steel frames subjected to near-fault ground motion excitations. *Int J Optim Civil Eng* 2019; **9**:177–93.
8. Nabati M, Gholizadeh S. Performance-based optimization of steel moment frames by a modified newton metaheuristic algorithm. *Int J Optim Civil Eng* 2023; **13**: 177–88.
9. Gholizadeh S, Hasançebi O, Eser H, Koçkaya O. Seismic collapse safety based optimization of steel Moment-Resisting frames. *Structures* 2022;**237**:112207.
10. Ghaderi M, Gholizadeh S. Mainshock–aftershock low-cycle fatigue damage evaluation of performance-based optimally designed steel moment frames. *Eng Struct* 2021;**237**:112207.
11. Kaveh A, Talatahari S. A charged system search with a fly to boundary method for discrete optimum design of truss structures. *Asian J Civil Eng*, 2010; **11**: 277–293.
12. Kaveh A, Talatahari S. An enhanced charged system search for configuration optimization using the concept of fields of forces. *Struct Multidiscip Optim*, 2011; **43**: 339–51.
13. Kaveh A, Mirzaei B, Jafarvand A. An improved magnetic charged system search for optimization of truss structures with continuous and discrete variables. *Appl Soft Comput*, 2015; **28**: 400–10.
14. Gholizadeh S, Ebadijalal M. Performance based discrete topology optimization of steel braced frames by a new metaheuristic. *Adv Eng Softw* 2018; **123**: 77–92.
15. Wen YK, Kang YJ. Minimum building life-cycle cost design criteria. I: Methodology. *J Struct Eng* 2001; **127**: 330–37.
16. Wen YK, Kang YJ. Minimum building life-cycle cost design criteria. II: Applications. *J Struct Eng* 2001; **127**: 338–46.
17. Mitropoulou CC, Lagaros ND, Papadrakakis M. Building design based on energy dissipation: a critical assessment. *Bull Earthq Eng* 2010; **8**: 1375–96.
18. Nikellis A, Sett K, Whittaker AS. Multihazard design and cost-benefit analysis of buildings with special moment–resisting steel frames. *J Struct Eng* 2019; **145**: 04019031.
19. Romano E, Cascini L, D'Aniello M, Portioli F, Landolfo R. A simplified multi-performance approach to life-cycle assessment of steel structures. *Structures* 2020; **27**: 371–82.
20. FEMA-350. Recommended seismic design criteria for new steel moment-frame buildings. Washington (DC): Federal Emergency Management Agency; 2000.
21. FEMA-P695. Quantification of building seismic performance factors. Washington (DC): Federal Emergency Management Agency; 2009.
22. ANSI/AISC 360-16. Specification for Structural Steel Buildings. American Institute of Steel Construction. Chicago, Illinois, 2016.
23. ASCE/SEI-41-13. Seismic Evaluation and Retrofit of Existing Buildings. American Society of Civil Engineers. Standard 41-13, 2014.
24. ANSI/AISC 341-16. Seismic Provisions for Structural Steel Buildings. American Institute of Steel Construction. Chicago, Illinois, 2016.

[DOI: 10.22068/ijoce.2024.14.3.604]

25. Fragiadakis M, Lagaros ND, Papadrakakis M. Performance-based multiobjective optimum design of steel structures considering life-cycle cost. *Struct Multidisc Optim* 2006; **32**: 1–11.
26. Gholizadeh S, Hasançebi O. Efficient neural network-aided seismic life-cycle cost optimization of steel moment frames. *Comput Struct* 2024; **301**: 107443.
27. ATC-13, Earthquake damage evaluation data for California. Applied Technology Council, Redwood City, 1985.
28. Elenas A, Meskouris K. Correlation study between seismic acceleration parameters and damage indices of structures. *Eng Struct* 2001; **23**: 698–704.
29. Standard No. 2800. Iranian Code of Practice for Seismic Resistant Design of Buildings, Building and Housing Research Center, Tehran, 2014.
30. *OpenSees*. Open System For Earthquake Engineering Simulation. ver 3.3.0 [Computer software]. PEER, Berkeley, CA.
31. NIST GCR 17-917-46v2. Guidelines for Nonlinear Structural Analysis for Design of Buildings. Part IIa – Steel Moment Frames. Applied Technology Council, 2017.

[DOI: 10.22068/ijoce.2024.14.3.604]